CILIARY MECHANISMS

A look under the hood of the machine that makes cilia beat

The central apparatus regulates the beating of motile cilia. High-resolution structures of the almost complete central apparatus are now reported in two separate studies, shedding light on the mechanism of ciliary beating and marking a new era in our molecular understanding of cilia architecture and function.

Elena A. Zehr and Antonina Roll-Mecak

The cilium is a microtubule-based organelle that protrudes from the apical surface of eukaryotic cells. It allowed early eukaryotic cells to move around, survive and reproduce. Many of the ciliary components can be traced all the way back to the proto-eukaryote. Antonie van Leeuwenhoek discovered cilia in 1677 and described them as "little feet" on the protists he examined with his microscope[1]. There are two types of cilia: non-motile or primary cilia, and motile cilia. Primary cilia function as a cell's antennae to sense external cues such as growth factors, fluid flow and developmental morphogens, and are essential for embryonic patterning and organogenesis. Motile cilia function to move extracellular fluid around tissues, for example, around the respiratory epithelium. In single-celled eukaryotes such as the biflagellate *Chlamydomonas reinhardtii*, a model organism for the study of cilia, or in monoflagellated sperm, the motile cilium's structurally identical flagellum is used for propulsion.

Despite their central role in biology, the molecular structure and even the exact protein composition of motile cilia are still not well-characterized. More than 600 proteins were assigned as being part of the flagella in *C. reinhardtii*[2], a model organism for the study of cilia. Motile cilia and eukaryotic flagella contain at their core a cylindrical, cartwheel-like structure called the axoneme (Fig. 1a, b). The axoneme is composed of a microtubule doublet (C1 and C2) at its center called the central pair. This central pair is missing in non-motile cilia. C1 and C2 outer surfaces are decorated by proteinaceous protrusions that connect C1 and C2 to each other, forming what is called the central bridge. Additional protrusions, known as projections, connect the central pair to peripheral axonemal components. Together, C1, C2, the central bridge, and the projections form the central apparatus (CA). The *C. reinhardtii* CA has six projections

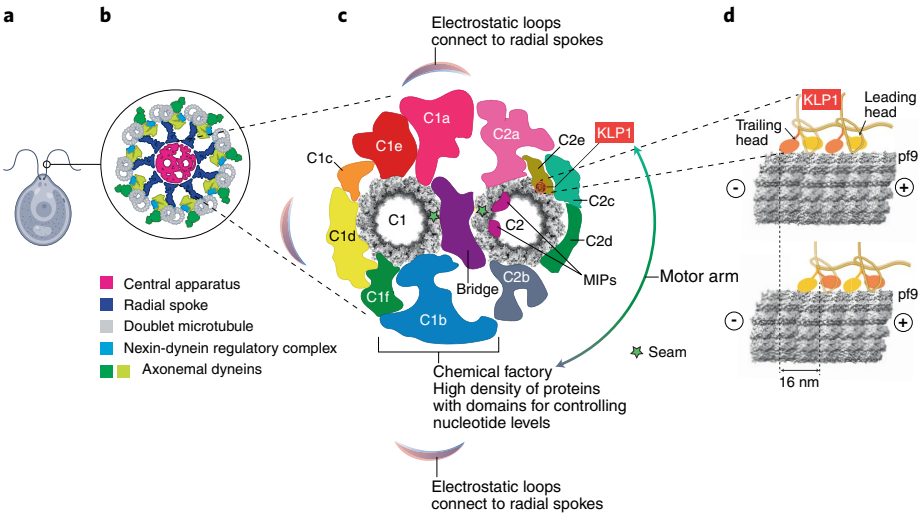

Fig. 1 | The central apparatus of motile cilia. a, The biflagellate *Chlamydomonas reinhardtii*, a model organism for the study of cilia. **b**, Structural organization of the axoneme. **c**, Structural organization of the central apparatus. The position of the seam is indicated by a star. **d**, An array of kinesin-like protein 1 (KLP1) dimers in two different stepping states shifted by 16 nm on microtubule protofilament 9 (pf9). MIPs, microtubule inner proteins. Figure adapted with permission from refs. [11,12], SpringerNature.

on the C1 microtubule and five on the C2 microtubule. The projections on C1 and C2 are numbered counter-clockwise, C1a-e-c-d-f-b, and clockwise, C2a-e-c-d-b, respectively (Fig. 1c). The CA is connected to nine peripheral doublet microtubules through elongated protein assemblies, called radial spokes. The peripheral microtubule doublets are bound to two sets of minus-end-directed dynein motors, the inner- and outer-arm dyneins (Fig. 1b), which generate the mechanical forces required for ciliary beating. Mutations in CA result in primary cilia dyskinesia, male infertility, and hydrocephalus[3,4].

Genetic, proteomic, and structural studies mapped proteins to the CA[5–9], but a complete, detailed view of the CA has been elusive. The complex organization and structural flexibility of CA components were major obstacles in obtaining high-resolution structures of the CA. Previous best-resolved cryo-electron microscopy (cryo-EM) maps of the CA from *C. reinhardtii* were limited to ~2 nm overall resolution[8,10] and did not permit direct mapping of many CA components. These components were located using nanogold-labelling combined with genetic deletions followed by cryo-EM reconstructions of the mutants. These studies succeeded in assigning protein components within the C1a-e-c and C1b projections, providing a partial molecular view of the CA, and explained how these components contribute to the structural integrity and assembly of the CA.

In this issue of *Nature Structural & Molecular Biology*, two impressive independent studies by Gui et al.[11]. and Han et al.[12]. report high-resolution tomographic

reconstructions (local resolution ranges from 3.0 Å to 6.0 Å) and almost complete atomic models of the CA. Key to obtaining the high-resolution maps was the analysis of carefully selected areas within the CA filaments coupled with novel approaches for data processing and model building. Specifically, manual selection of straight CA regions that were amenable to averaging and focused refinement of separate components of the CA helped to overcome the problems posed by structural flexibility within this large complex. To identify CA components and then build de novo atomic models the authors combined manual model building with automatic deep-learning protein-fold recognition and atomic model building, as well as reconstruction of the CA from a *C. reinhardtii* mutant.

The high-resolution structures of the CA allowed the authors to precisely map the arrangement and interactions of the microtubule inner and outer surface proteins (MIPS and MOSPs, respectively) bound to the central microtubule doublet. MIPs, which reside inside the microtubule lumen[9], remodel individual tubulin subunits and create extensive networks stabilizing the microtubule. MIPs seem to be a staple of microtubule structures that need to withstand large forces, such as axonemal microtubules. Many of the MIPs follow the contours of the microtubule lattice and lack globular domains. Gui et al. describe two major classes of MIPs: the SAXO (stabilizers of axonemal microtubules) proteins, and the arc-MIPs. SAXO proteins run longitudinally on the microtubule and bind at the lateral interface between protofilaments, stabilizing the microtubule. Arc-MIPs bind at the interface between α–β-tubulin dimers and run along the length of multiple protofilaments in an arc, thus also gluing protofilaments to each other and possibly decreasing inter-protofilament shearing. MIPs bind to luminal loops that play important roles in stabilizing the microtubule. For example, several MIPs bind and stabilize the K40-loop of α-tubulin. K40 is acetylated in cilia[13] and is involved in tuning lateral contacts between protofilaments[14]. In the absence of MIPS, the K-40 loop is disordered[14]. MIPs in the outer microtubule doublet also bind and stabilize the K-40 loop[15]. It is unclear whether acetylation at this site is important for the recruitment of the MIPs. This will likely be a topic of future work, as cilia grow slower in the absence of the K-40 acetylation. MIPs also bind and remodel the M-loop of β-tubulin, which participates in lateral contacts between protofilaments and is part of the binding site for taxol, a drug that stabilizes microtubules[16]. Almost 90% of the taxol-binding pockets in C1 and C2 are occupied by MIPs, highlighting the key role of the M-loop region in regulating microtubule stability. Outer doublet microtubules also have MIPs bound to their M-loops[17]. MOSPs include what the authors call a 'spring layer', formed of armadillo repeats, to which the projections are attached through ASH (ASPM, SPD-2, Hydin) proteins. The spring layer's key component is PF16, which forms discontinuous right-handed spirals around the outer surface of the C1 microtubule and is the foundation upon which all C1 projections are built. This arrangement explains why *pf16* mutants are characterized by unstable C1 and abnormal flagellar movement[6]. The specificity for establishing each projection over the homotypic PF16 networks is determined by the ASH proteins, which tether PF16 to specific protofilaments on the C1 microtubule by recognizing composite features on the microtubule surface, including other microtubule binding proteins. Intriguingly, differences in curvature between protofilaments might also play a role in specifying the sites of interaction as both groups observe a larger variability in inter-protofilament angles in CA microtubules than observed on naked microtubules assembled in vitro. This observation raises the question of whether changes in protofilament angles, induced possibly by MIP binding, can control the stepwise recruitment of CA components. The absence of specific ASH proteins results in selective loss of one or more projections[4]. ASH proteins are also part of the flexible bridge that tether C1 and C2 to each other (Fig. 1c). The projections on C1 with 16- and 32-nm periodicities are determined by FAP194, which establishes regular connections to C2 and matches the distance between the radial spokes. The 16-nm periodicity on the C2 outer surface is determined by PF20. The globular domain of PF20 binds the C2 seam (Fig. 1c), while its coiled coils run perpendicular to the microtubule long axis to anchor the C2a projection. The microtubule seam is characterized by non-canonical heterotypic lattice interactions between α–β-tubulin dimers and thus offers a unique binding interface for proteins. PF20 is also part of the bridge connecting C1 and C2, explaining why *pf20* mutants miss the entire CA and have paralyzed flagella[18]. The authors propose that PF20 plays an essential role in positioning the C1 and C2 microtubules by recognizing the seam. The atomic model of the CA also reveals intricate proteinaceous networks at the distal ends of the projections that connect projections to each other, as well as to the radial spokes. The authors of the two studies propose that the electrostatic loops at the distal ends of the C1a-e-d-b projections interact with the radial spokes and that this interaction allows the transmission of mechanical signals from the CA to the periphery of the axoneme (Fig. 1c).

The CA structures also reveal elongated rachis-like proteins within projections that functionally organize the projections' components. Interestingly, the rachis-like protein of the C1b projection, CPC1, has an adenylate kinase domain that potentially regulates ATP levels[19] and organizes a cluster of proteins that either produce or consume ATP. This suggests that the C1b projection is the "chemical factory" that regulates nucleotide levels within the flagellum and thus modulates the activity of outer-doublet-bound dynein motors. This chemical factory is near the motile region consisting of C2b-c-d-e, called the motor arm (Fig. 1c), which slides along the C2 microtubule. The motor arm is attached to C2 via the kinesin-like protein, KLP1, which is important for the integrity of the C2b, C2d and C2c projections and flagellar beating[9,20]. Han et al. were able to resolve the array of KLP1 dimers along protofilament 9 of C2 in two different stepping states, shifted from one another by 16 nm along the protofilament. The trailing head of KLP1 is docked to the microtubule, while its leading head is in an undocked conformation (Fig. 1d). The motors are linked in an array via their tail domains and accessory proteins. The array of kinesins, powered by the ATP factory nearby, facilitates the sliding of the flexibly linked C1 and C2 against each other. The structural changes of the CA are then transmitted via the projections and radial spokes to the periphery of the axoneme regulating the conformation of the outer doublets and, ultimately, the whole flagellum. The exact mechanism of how the structural changes in the CA are transmitted to the outer doublets remains to be explored.

Previous cryo-EM studies revealed the architecture of the nine outer doublets decorated with dynein motors and how these dynein motors power the sliding of the microtubules needed for flagella and cilia beating[15,21–25]. The structures of the CA, the core of the motile cilia, reported by Gui et al. and Han et al. in this issue significantly expand our understanding of cilia by identifying many novel CA proteins and revealing the assembly principles of this magnificent machine and how it connects to the outer doublets. These studies contribute textbook knowledge to cilia biology and bring us one step closer to having high-resolution structures of the whole axoneme, more than three centuries after Leeuwenhoek marveled at the fluttering cilia

on the protists from a puddle of rainwater. The next challenge is to understand the kinetics and fidelity of assembly of this large molecular machine and visualize at high resolution the conformational transitions during ciliary beating and how these are tuned in cells with diverse waveforms. ❐

Elena A. Zehr[1]✉ and Antonina Roll-Mecak[1,2]✉

[1]*Cell Biology and Biophysics Unit, National Institute of Neurological Disorders and Stroke, Bethesda, MD, USA.* [2]*Biochemistry and Biophysics Center, National Heart, Lung and Blood Institute, Bethesda, MD, USA.*

✉*e-mail: Elena.Zehr@nih.gov; Antonina@nih.gov*

Published online: 16 May 2022
https://doi.org/10.1038/s41594-022-00778-8

References

1. Leewenhoeck, A. *Philos. Trans.* **12**, 821–831 (1677).
2. Pazour, G. J., Agrin, N., Leszyk, J. & Witman, G. B. *J. Cell Biol.* **170**, 103–113 (2005).
3. Sapiro, R. et al. *Mol. Cell Biol.* **22**, 6298–6305 (2002).
4. Lechtreck, K. F., Delmotte, P., Robinson, M. L., Sanderson, M. J. & Witman, G. B. *J. Cell Biol.* **180**, 633–643 (2008).
5. Witman, G. B., Plummer, J. & Sander, G. *J. Cell Biol.* **76**, 729–747 (1978).
6. Dutcher, S. K., Huang, B. & Luck, D. J. *J. Cell Biol.* **98**, 229–236 (1984).
7. Zhao, L., Hou, Y., Picariello, T., Craige, B. & Witman, G. B. *J. Cell Biol.* **218**, 2051–2070 (2019).
8. Fu, G. et al. *J. Cell Biol.* **218**, 4236–4251 (2019).
9. Carbajal-González, B. I. et al. *Cytoskeleton* **70**, 101–120 (2013).
10. Cai, K. et al. *J. Cell Sci.* **134**, jcs254227 (2021).
11. Gui, M., Wang, X., Dutcher, S. K., Brown, A. & Zhang, R. *Nat. Struct. Mol. Biol.* https://doi.org/10.1038/s41594-022-00770-2 (2022).
12. Han, L. et al. *Nat. Struct. Mol. Biol.* https://doi.org/10.1038/s41594-022-00769-9 (2022).
13. Roll-Mecak, A. *Dev. Cell* **54**, 7–20 (2020).
14. Eshun-Wilson, L. et al. *Proc. Natl Acad. Sci. USA* **116**, 10366–10371 (2019).
15. Ma, M. et al. *Cell* **179**, 909–922.e12 (2019).
16. Kellogg, E. H. et al. *J. Mol. Biol.* **429**, 633–646 (2017).
17. Ichikawa, M. et al. *Proc. Natl Acad. Sci. USA* **116**, 19930–19938 (2019).
18. Smith, E. F. & Lefebvre, P. A. *Mol. Biol. Cell* **8**, 455–467 (1997).
19. Mitchell, B. F., Pedersen, L. B., Feely, M., Rosenbaum, J. L. & Mitchell, D. R. *Mol. Biol. Cell* **16**, 4509–4518 (2005).
20. Yokoyama, R., O'Toole, E., Ghosh, S. & Mitchell, D. R. *Proc. Natl Acad. Sci. USA* **101**, 17398–17403 (2004).
21. Grossman-Haham, I. et al. *Nat. Struct. Mol. Biol.* **28**, 20–28 (2021).
22. Bui, K. H., Yagi, T., Yamamoto, R., Kamiya, R. & Ishikawa, T. *J. Cell Biol.* **198**, 913–925 (2012).
23. Heuser, T. et al. *Proc. Natl Acad. Sci. USA* **109**, E2067–E2076 (2012).
24. Rao, Q. et al. *Nat. Struct. Mol. Biol.* **28**, 799–810 (2021).
25. Lin, J. & Nicastro, D. *Science* **360**, eaar1968 (2018).

Acknowledgements

A.R.-M. is supported by the intramural programs of the National Institute of Neurological Disorders and Stroke (NINDS) and National Heart, Lung, and Blood Institute (NHLBI).

Competing interests

The authors declare no competing interests.